CrystEngComm

PAPER

View Article Online
View Journal | View Issue

Cite this: *CrystEngComm*, 2023, **25**, 3013

Host behaviour of two tricyclic fused systems in mixed anisole guest solvents†

Benita Barton, * Danica B. Trollip and Eric C. Hosten

Two tricyclic fused host systems, namely *N*,*N*′-bis(5-phenyl-5-dibenzo[*a*,*d*]cycloheptenyl)ethylenediamine **H1** and *N*,*N*′-bis(5-phenyl-10,11-dihydro-5-dibenzo[*a*,*d*]cycloheptenyl)ethylenediamine **H2**, were recrystallized from each of anisole and 2-, 3- and 4-methylanisole (ANI, 2MA, 3MA and 4MA), and it was observed that **H1** formed complexes with 2MA (host : guest 2 : 1), 3MA (1 : 1 at 4 °C) and 4MA (1 : 1), while **H2** only enclathrated ANI (2 : 3). Mixed solvent competition experiments using **H1** revealed this host compound to possess a remarkable affinity for 4MA; in fact, complexation was only successful if this guest compound was present in the mixture. Similar experiments but with **H2** were, unfortunately, not enlightening owing to the fact that crystals did not form in these conditions. SCXRD experiments showed that the affinity of **H1** for 4MA relative to 3MA was as a result of intermolecular host···host C–H···π and π···π interactions in **H1**·4MA that were significantly shorter than in **H1**·3MA which, in turn, led to a higher crystal density for **H1**·4MA (1.215 g cm^{-1}) compared with **H1**·3MA (1.184 g cm^{-1}), despite their identical chemical formulae. Thermal analyses showed that the guest molecules in **H1**·4MA also escaped from the crystals at a higher temperature (104.9 °C) than that in **H1**·3MA (70.5 °C). Unfortunately, from selectivity coefficient (*K*) calculations, **H1** would not be able to serve as an ideal host candidate for the separations of these anisole mixtures.

Received 21st February 2023,
Accepted 30th March 2023

DOI: 10.1039/d3ce00174a

rsc.li/crystengcomm

1. Introduction

Anisole (ANI)[1] and its *C*-methylated derivatives (methylanisoles 2MA, 3MA and 4MA) (Scheme 1) have a broad range of applications in chemicals based industries, and examples include their employment as building blocks in the preparation of pharmaceutical products, pheromones and perfumes, to mention a few only.[2] Additionally, ANI and 4MA can be found in trace amounts in certain natural products and crop oils.[3] Alkylation using methanol is one of the more common methods used to transform phenol to ANI, and the different *o*-, *m*- and *p*-cresols to the MAs.[2,4] In the case of the synthesis of the MAs, phenol may be subjected to *O*-alkylation to form ANI following which ANI then reacts through *C*-alkylation to form the MA compound.[5] However, these reactions oftentimes lead to a mixture of ANI and isomeric MA products. While ANI may readily be removed from the mixture through distillation processes owing to its different boiling point (153.8 °C), the MAs are not as readily separated into their pure constituents as a result of their very similar boiling points (171.0, 175.5 and 175.5 °C for 2MA, 3MA and 4MA, respectively).[6] As such, fractional distillations and/or crystallizations for these separations present a challenge and, therefore, there exists a need to discover separation techniques that are more facile and efficient, and less costly than these more conventional means.

It has long been recognized that host–guest chemistry may serve as a separatory strategy for such isomeric mixtures.[7–11] Zhang[12] and Barbour[13] and their co-workers considered the separation of the xylenes by employing a cucurbit[7]uril host macrocycle and a Werner complex containing nickel, respectively, with much success. Similarly, Nassimbeni *et al.*[14] revealed the likelihood of using two fluorenyl diol host compounds for the separation of methylated piperidines. In our own laboratories, *trans*-9,10-dihydro-9,10-ethanoanthracene-11,12-dicarboxylic acid and (*R*,*R*)-(−)-2,3-dimethoxy-1,1,4,4-tetraphenylbutane-1,4-diol were presented with the mixed anisole guest compounds and were revealed to possess enhanced selectivities for 4MA and ANI, respectively.[15,16]

Host–guest chemistry is that field of science that falls into the broader supramolecular chemistry area, and successful separations of isomers rely upon the appointed host compound displaying selectivity for one particular guest when presented with isomeric mixtures. This, in turn, is more usually reliant on noncovalent interactions between the host and guest species to

Department of Chemistry, Nelson Mandela University, PO Box 77000, Port Elizabeth, 6031, South Africa. E-mail: benita.barton@mandela.ac.za

† The crystallographic data for **H1**·3MA, **H1**·4MA and 2(**H2**)·3(ANI). CCDC 2242822, 2167904 and 2241513. For crystallographic data in CIF or other electronic format see DOI: **https://doi.org/10.1039/d3ce00174a**

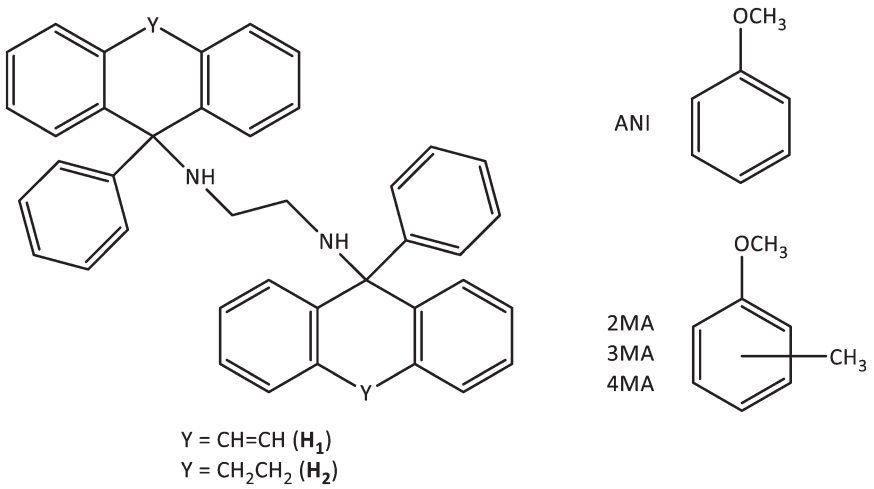

Scheme 1 Host compounds *N*,*N*′-bis(5-phenyl-5-dibenzo[*a*,*d*]cycloheptenyl)ethylenediamine **H1** and *N*,*N*′-bis(5-phenyl-10,11-dihydro-5-dibenzo[*a*,*d*]cyclohep-tenyl)ethylenediamine **H2**, together with the proposed guest solvents anisole (ANI) and 2-, 3- and 4-methylanisole (2MA, 3MA, 4MA).

furnish stable complexes (also known as inclusion compounds) with optimal host–guest packing modes. The list of the possible contact types between the different species is extensive, and the more important interactions include both classical and nonclassical hydrogen bonding, C–H···π interactions and π···π stacking, depending, naturally, on the functional groups present in the molecules.[17,18]

The two tricyclic-fused host systems, *N*,*N*′-bis(5-phenyl-5-dibenzo[*a*,*d*]cycloheptenyl)ethylenediamine **H1** and its 10,11-dihydro analogue *N*,*N*′-bis(5-phenyl-10,11-dihydro-5-dibenzo[*a*,*d*]cycloheptenyl)ethylenediamine **H2** (Scheme 1), have been used with tremendous effect for the separation of various mixtures containing the xylenes (*o*-Xy, *m*-Xy and *p*-Xy) and/or ethylbenzene.[19] In that work, **H1** and **H2** possessed significant selectivities for *p*-Xy and *o*-Xy, respectively. These host compounds, while having the ability to form inclusion compounds with a wide variety of guest species, were found also to have an affinity for small dihalogenated alkanes.[20] As a result of their complexation abilities, it was deemed appropriate to investigate their separation potential for mixtures containing two or more of ANI, 2MA, 3MA and 4MA. Where possible, single crystal diffraction analyses (SCXRD) were employed to identify the various inter- and intramolecular interactions in successfully prepared complexes as well as thermal analyses to determine complex stabilities, and these results were related back to any affinities displayed by each host compound. We report on these observations now.

2. Experimental

2.1 General

All starting and guest compounds were purchased from Merck and were used without further modification.

^{1}H-NMR experiments were carried out by means of a Bruker Ultrashield Plus 400 MHz spectrometer; $CDCl_3$ was the deuterated dissolution solvent.

Three GC (gas chromatography) instruments were employed, dependent upon availability (the applicable column was an Agilent J&W Cyclosil-B column (30 m × 250 μm × 0.25 μm)). The first was a Young Lin YL6500 GC, and the method involved an initial temperature hold time for a minute at 50 °C, which was then heated at a rate of 10 °C min^{-1} until a final temperature of 110 °C was reached; this was held there for 4 min. The split ratio and flow rate were altered from 1 : 80 to 1 : 20 and 1.5 to 1.7 and then back to 1.5 mL min^{-1}, respectively (the split ratio was varied in order to increase the intensity of the peaks on the chromatogram, while the flow rate was changed in order to improve separations between the peaks). The second employed an Agilent Technologies 7890A GC instrument and the method commenced with an initial temperature of 50 °C that was held for 1 min, followed by a heating rate of 10 °C min^{-1} until 110 °C was reached; this temperature was maintained for 3 min. The flow rate of the column had fluctuations between 1 and 1.5 mL min^{-1} due to the column pressure changing at times. The split ratio was 1 : 80. The third method used an Agilent Technologies 6890N GC instrument. An initial temperature of 50 °C was held for 1 min, followed by a heating rate of 10 °C min^{-1} until 110 °C was reached, and this temperature was maintained for 2 min. The flow rate and split ratio were 1.5 mL min^{-1} and 1 : 80, respectively.

Complexes with suitable crystal quality were analysed by means of SCXRD experiments. Intensity data for **H1**·3MA, **H1**·4MA and 2(**H2**)·3(ANI) were obtained at 296, 200 and 296 K, respectively, by means of a Bruker Kappa Apex II diffractometer with graphite-monochromated MoKα radiation (λ = 0.71073 Å). APEXII was used for data-collection while SAINT was employed for cell refinement and data reduction.[21] SHELXT-2018/2 (ref. 22) was used to solve the structures, and these were refined by means of least-squares procedures using SHELXL-2018/3 (ref. 23) together with SHELXLE[24] as a graphical interface. All non-hydrogen atoms

were refined anisotropically, while the carbon-bound hydrogen atoms were inserted in idealized geometrical positions in a riding model; nitrogen-bound hydrogens were found on the difference map and were then allowed to refine freely. Data were corrected for absorption effects using the numerical method implemented in SADABS.[21] The PLATON/SQUEEZE routine showed that both crystal structures **H1**·3MA and **H1**·4MA showed full occupancy. The crystallographic data for **H1**·3MA, **H1**·4MA and 2(**H2**)·3(ANI) were deposited at the Cambridge Crystallographic Data Centre (CCDC) and their CCDC numbers are 2242822, 2167904 and 2241513.

Thermoanalytical experiments were carried out on all of the single solvent complexes prepared in this work. For these analyses, after recovery of the solids from the glass vials by means of vacuum filtration and washing with petroleum ether (40–60 °C), the crystals were patted dry in folded filter paper and then analysed directly without further manipulation. The instrumentation used was either a TA SDT Q600 (with the data analysed using TA Universal Analysis 2000 software) or a Perkin Elmer STA6000 Simultaneous Thermal Analyser (with the data analysed by means of Perkin Elmer Pyris 13 Thermal Analysis software). The samples were placed in open ceramic pans while an empty ceramic pan functioned as the reference. The purge gas was high purity nitrogen. The samples were heated from approximately 40 to 400 °C (for the TA SDT Q600 module system) and from 40 to 340 °C (for the Pyris system) with a heating rate of 10 °C min^{-1}.

2.2 Synthesis of H1 and H2

Both host compounds **H1** and **H2** were prepared by considering a previous report.[20]

2.3 Single solvent recrystallization experiments

The host compounds were recrystallized from each of the four anisole solvents in order to determine whether they possessed any enclathration abilities for these organic solvents. Therefore, **H1** (0.05 g, 0.08 mmol) and **H2** (0.04 g; 0.07 mmol) were dissolved in an excess of each of these anisoles (10 mmol). The glass vials in which these experiments were conducted were then closed and placed in the cold room (4 °C) which facilitated crystallization. The crystals were collected by means of vacuum filtration, crushed and washed with petroleum ether (40–60 °C), and then analysed by means of ^{1}H-NMR spectroscopy. This analytical technique assisted in determining if complexation had occurred and, if so, the host : guest (H : G) ratio of each complex was calculated through comparisons of the integrals of relevant host and guest resonance signals.

2.4 Equimolar mixed guest solvent recrystallization experiments

The selectivity behaviour of the host compounds was evaluated by dissolving **H1** (0.05 g, 0.08 mmol) and **H2** (0.04 g, 0.07 mmol) in equimolar mixtures of the anisole guests (7 mmol combined amount for **H1**, with an additional 10 drops of benzene to aid dissolution, and 10 mmol combined amount for **H2**). All possible guest combinations were considered, and thus binary, ternary and quaternary mixed solvents were prepared in this way. The vials were closed and stored in the cold room (4 °C), and the crystals that formed in this way were collected by suction filtration, washed with petroleum ether (40–60 °C) or methanol (when no petroleum ether was available), and analysed by means of GC to obtain the guest ratios in the mixed complexes. ^{1}H-NMR spectroscopy was employed to obtain the overall H : G ratios.

2.5 Recrystallization experiments involving binary guest mixtures in varying molar ratios

The selectivity behaviour of each host compound was assessed in binary guest mixtures where the guest : guest (G : G) molar ratios were varied between approximately 80 : 20 and 20 : 80 for guests A (G_A) and B (G_B), respectively. The host compounds **H1** (0.05 g, 0.08 mmol) and **H2** (0.04 g, 0.07 mmol) were dissolved in these solutions (combined amount of 7 mmol for **H1**, with an added 20 drops of benzene, and 10 mmol combined amount for **H2**), the vials closed and stored in the cold room (4 °C). Upon crystallization in these conditions, the crystals were recovered and treated as in the equimolar experiments, and the G : G ratios in each of the so-formed crystals (Z) quantified by means of GC to determine the G_A : G_B molar ratios in this phase. Selectivity profiles were then constructed by plotting Z for G_A (or G_B) against X for G_A (or G_B) (where X is the amount of G_A (or G_B) in the original solution). These profiles allowed a visual depiction of the host selectivity behaviour as the guest concentrations varied. The selectivity coefficient, $K_{G_A:G_B}$, which was obtained by using the equation $K_{G_A:G_B} = Z_{G_A}/Z_{G_B} \times X_{G_B}/X_{G_A}$, where $X_{G_A} + X_{G_B} = 1$, served as a measure of the selectivity of each host compound in these conditions.[25] $K_{G_A:G_B} = 1$ when the host compound possesses no selectivity, and the straight lines in these plots represent this instance.

2.6 Software

Software program Mercury was employed in order to construct unit cell diagrams as well as host–guest packing figures.[26] Also by means of this program were prepared void diagrams: here, the guest molecules were first deleted from the packing diagram, and then the voids were calculated and displayed after analysing the spaces that remained with a probe that had a 1.2 Å radius. A scrutiny of these latter diagrams revealed the nature of the guest accommodation, whether in discrete cages or in channels.

3. Results and discussion

3.1 Single solvent recrystallization experiments

Table 1 contains the results obtained after crystals were isolated from the single solvent recrystallization experiments and after ^{1}H-NMR analyses were conducted on these.

Table 1 Recrystallization experiments of **H1** and **H2** from each of ANI, 2MA, 3MA and 4MA

Guest	**H1** : G[a]	**H2** : G[a]
ANI	1 : 0	2 : 3
2MA	2 : 1	[b]
3MA	1 : 0 (RT[c]); 1 : 1 (4 °C)	[b]
4MA	1 : 1	[b]

[a] Host : guest (H : G) ratios were determined using ^{1}H-NMR spectroscopy. [b] No crystallization occurred. [c] Room temperature.

Table 1 shows that both host compounds have complexation ability for some of the anisole guest solvents. **H1** included 2MA and 4MA with 2 : 1 and 1 : 1 host : guest (H : G) ratios while the complexation of this host compound with 3MA depended upon the temperature at which the recrystallization experiment was conducted: at room temperature (RT), no inclusion occurred but at lower temperatures (4 °C), a 1 : 1 complex was isolated. ANI did not form an inclusion compound with **H1**. **H2**, on the other hand, only formed a complex with ANI (H : G 2 : 3); gels remained in the glass vials for the 2MA, 3MA and 4MA experiments and no crystals formed in these three instances.

3.2 Equimolar mixed guest solvent recrystallization experiments

Table 2 summarizes the results obtained from competition experiments when host compound **H1** was recrystallized from equimolar binary, ternary and quaternary mixtures of ANI, 2MA, 3MA and 4MA. Unfortunately, analogous experiments with **H2** presented immense challenges: these experiments almost always resulted in gels, with no crystals forming in the vials, and so the results for these experiments could not be obtained.

In Table 2, the preferred guest is indicated in bold black text for each individual competition experiment, and the percentage estimated standard deviations (%e.s.d.s) are provided in parentheses, calculated as a result of the fact that each experiment was conducted in duplicate.

From this table (Table 2), no inclusion occurred in the binary experiments ANI/2MA, ANI/3MA and 2MA/3MA, and only apohost was recovered from the glass vials in these instances. In fact, remarkably, only when the solutions contained 4MA was complexation with **H1** successful. The binary experiments ANI/4MA, 2MA/4MA and 3MA/4MA afforded crystals with significant amounts of 4MA (91.7, 89.3 and 84.4%, respectively), and this guest was thus undoubtedly overwhelmingly preferred in these guest/guest competition experiments.

From the ternary equimolar experiments comprising ANI/2MA/4MA, ANI/3MA/4MA and 2MA/3MA/4MA, the host affinity for 4MA persisted in these conditions, and recovered crystals contained 66.3, 75.0 and 75.9% 4MA, respectively. Once more, when 4MA was absent (ANI/2MA/3MA), only apohost compound was recovered.

Finally, the equimolar experiment in which all four guest solvents were present resulted in a mixed complex with an elevated quantity of 4MA once more (68.9%). From this particular experiment, the host selectivity was thus in the order 4MA (68.9%) $\gg$ 3MA (14.1%) $>$ 2MA (8.5%) $\approx$ ANI (8.5%).

In all successful complexation experiments, the overall H : G was consistently 1 : 1, with the exception of the quaternary mixture, where this ratio was 1 : 2.

3.3 Recrystallization experiments involving binary guest mixtures in varying molar ratios

The selectivity profiles that were obtained for **H1** by plotting Z for G_A (or G_B) against X for G_A (or G_B) after GC analyses of the crystals emanating from the binary solutions are provided in Fig. 1a–c (once more, comparable experiments with **H2** were not possible; crystallization was not successful). Note that if these binary solutions did not contain 4MA, only apohost was recovered from the glass vials in every case (as was also observed in the equimolar experiments) and no selectivity profiles could be constructed in these instances. The averaged K values (K_{ave}) for the three sets of binary experiments are summarised in Table 3.

Table 2 Complexes formed by **H1** in equimolar mixed anisole guests[a,b]

ANI	2MA	3MA	4MA	Guest ratios (%e.s.d.s)	Overall H : G ratio
X	*X*			[c]	[c]
X		*X*		[c]	[c]
X			***X***	8.3 : **91.7**(0.6)	1 : 1
	X	*X*		[c]	[c]
	X		***X***	10.7 : **89.3**(1.4)	1 : 1
		X	***X***	15.6 : **84.4**(1.4)	1 : 1
X	*X*	*X*		[c]	[c]
X	*X*		***X***	19.0 : 14.7 : **66.3**(2.6 : 2.0 : 4.6)	1 : 1
X		*X*	***X***	9.4 : 15.6 : **75.0**(2.1 : 0.4 : 1.7)	1 : 1
	X	*X*	***X***	9.1 : 15.0 : **75.9**(2.2 : 1.4 : 3.5)	1 : 1
X	*X*	*X*	***X***	8.5 : 8.5 : 14.1 : **68.9**(2.3 : 1.8 : 0.9 : 3.2)	1 : 2

[a] GC–MS and ^{1}H-NMR spectroscopy were used to obtain the G : G and overall H : G ratios, respectively. [b] The competition experiments were conducted in duplicate; the %e.s.d.s are provided in parentheses. [c] No inclusion occurred and only apohost was recovered from the experiment.

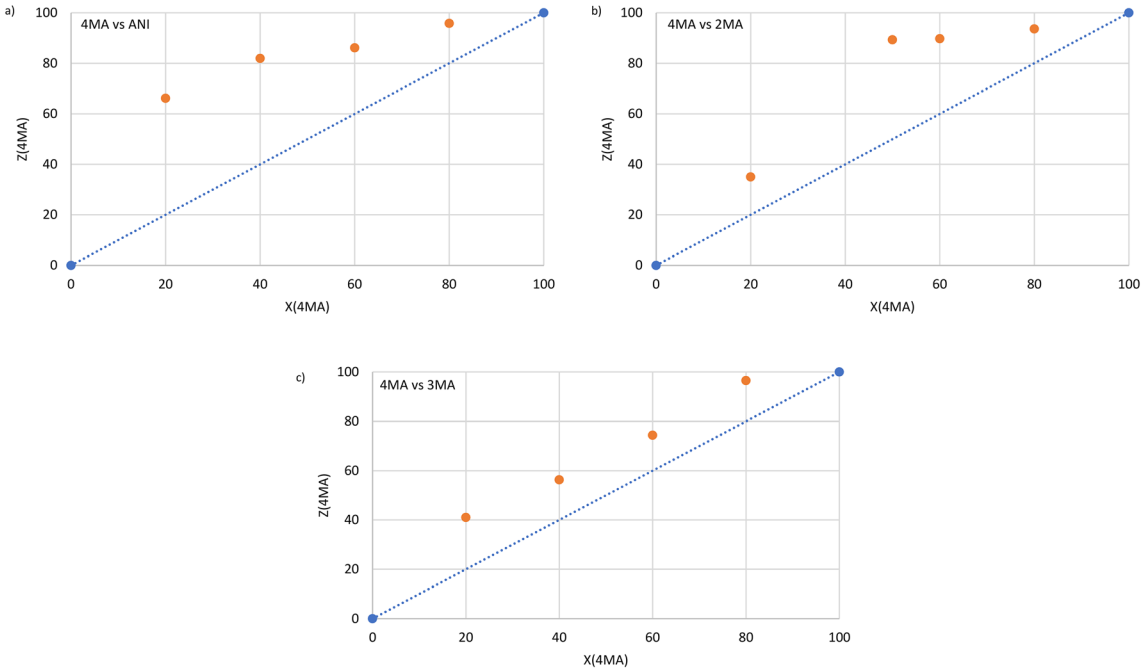

Fig. 1 Selectivity profiles of **H1** in a) 4MA/ANI, b) 4MA/2MA and c) 4MA/3MA binary solutions.

From Fig. 1a (4MA/ANI), it is clear that 4MA remained significantly preferred across the concentration range. This was true even at low concentrations (20%) of 4MA in the solution, where the recovered crystals then already contained 66.2% of this guest species. This particular experiment also furnished the highest selectivity coefficient (K = 6.8). When the solution contained 40% 4MA, the so-formed crystals were observed to have 81.9% 4MA, while the 60 : 40 and 80 : 20 (4MA/ANI) mixtures produced crystals that were significantly enriched with 4MA (86.1 and 95.8%, respectively). K_{ave} for this set of experiments was 6.1 (Table 3) and, in general, the individual K values were too low for the efficient separations of such mixtures, as suggested by Nassimbeni *et al.*, who stipulated that K should be 10 or greater for practically feasible separations.[27]

Fig. 1b (4MA/2MA) shows that 4MA was, once more, the favoured guest solvent throughout. Solutions with 20, 50, 60 and 80% 4MA afforded crystals that contained 35.0, 89.3, 89.7 and 93.6% of this guest solvent. The highest K value that was calculated was 8.3 and this was in the binary solution that contained equal molar quantities of each guest species, while K_{ave} was 5.0 in this set of experiments (Table 3). Once more, **H1** would not be able to effectively separate any of these mixtures.

Table 3 K_{ave} values for the binary guest competition experiments with **H1** in mixed anisoles

Binary mixture	K_{ave}
4MA/ANI	6.1
4MA/2MA	5.0
4MA/3MA	3.4

Once again, Fig. 1c (4MA/3MA) demonstrates that **H1** consistently selected for 4MA. The K values in these experiments ranged from a modest 1.9 to 6.7 and were calculated from experiments that had 4MA concentrations of 40 and 80%, respectively. The K_{ave} was, however, only 3.4 (Table 3). **H1** would, therefore, also not be able to effect the separation of these solutions.

Overall, the performance of **H1** was better in 4MA/ANI mixtures followed by 4MA/2MA and 4MA/3MA solutions, as observed from the K_{ave} values (6.1, 5.0 and 3.4%, Table 3). This was not entirely unexpected given the host selectivity order 4MA $\gg$ 3MA $>$ 2MA $\approx$ ANI as obtained from the equimolar experiments. Hence ANI and 2MA were not able to compete effectively with 4MA, whilst 3MA did offer some opposition. The K values, even for each individual data point in this work, were always, disappointingly, lower than 10, and so **H1** cannot be nominated as an ideal host candidate to successfully effect these anisole separations.

3.4 SCXRD experiments

Crystals of the single solvent complexes were analysed by means of SCXRD experiments with the exception of 2(**H1**)·2MA, which was recovered as a fine powder. In **H1**·3MA and **H1**·4MA, the guest molecules were disordered around an inversion point, while there were two guest molecules in the unit cell of 2(**H2**)·3(ANI): one ANI was also disordered around an inversion point while the second ANI molecule showed no disorder whatsoever.

A summary of the applicable crystallographic data for these SCXRD experiments is provided in Table 4. All three of the complexes crystallized in the triclinic crystal system and

space group $P\bar{1}$. Owing to the very similar unit cell dimensions for **H1**·3MA and **H1**·4MA, it was concluded that these two complexes shared a common host packing. In 2(**H2**)·3(ANI), however, this packing was unique.

Host–guest packing (left) and void (right) diagrams, prepared using software Mercury for each of the three complexes,[26] are provided in Fig. 2a–c for **H1**·3MA, **H1**·4MA and 2(**H2**)·3(ANI), respectively. It is clear from the first two of these (Fig. 2a and b) that the host packing in the complex containing 3MA and 4MA is indeed isostructural, and that both types of guest molecules were housed in wide open and infinite channels that were parallel to the *a*-axis. In the 3(**H2**)·2(ANI) complex, ANI was also housed in channels, but these were multi-directional (along both the *a*- and *c*-axes, Fig. 2c).

With the knowledge that the host packing in **H1**·3MA and **H1**·4MA was isostructural (and both enjoyed the same H : G ratios, 1 : 1, Table 1), it was deemed reasonable that one might expect 3MA and 4MA to compete effectively with one another for **H1** when present in mixtures. However, from Table 2, this was clearly not the case, and 4MA was overwhelmingly preferred in the binary equimolar mixture containing these two guests (84.4%). The question therefore arose as to why this was the case, why did 3MA not compete successfully with 4MA for the spaces in crystals of the complex if the host packing was isostructural. Clearly, the host packing with 4MA must have offered advantages compared to packing with 3MA. We therefore considered the densities of the crystals of **H1**·3MA and **H1**·4MA (Table 4) and found that these differed significantly from one another (1.184 and 1.215 g cm^{-1}, correspondingly). This, in itself, is noteworthy since the chemical formulae of the two complexes are identical (Table 4). Therefore, 3MA required more space for it to be included while 4MA used less space (as is expected given the more streamlined geometry of 4MA relative to 3MA). We therefore conclude that one of the reasons for the preference of **H1** for 4MA in 3MA/4MA mixtures was due to a more optimal (tighter) packing of the host molecules in that unit cell.

The noncovalent interactions in the two isostructural complexes (**H1**·3MA and **H1**·4MA) were subsequently compared. Each of the two complexes experienced one significant intermolecular (host)π···π(host) interaction between two aromatic moieties of the tricyclic fused ring systems (Fig. 3) and one intermolecular (host)C–H···π(host) contact (Fig. 4). These measured 3.645 (**H1**·3MA) and 3.636 Å (**H1**·4MA) (slippages were 0.833 and 0.822 Å, respectively), and 2.761 (**H1**·3MA) and 2.682 Å (**H1**·4MA) (H···π) (with both corresponding C–H···π angles being 151°). These π···π and C–H···π interactions in the latter complex were much shorter than in the former, and it is plausible that these shorter distances were responsible for the greater density of crystals of **H1**·4MA compared with **H1**·3MA, thus facilitating a tighter packing between the host molecules in the 4MA-containing complex. These observations therefore explain the preferential behaviour of **H1** towards 4MA compared with

Table 4 Crystallographic data for the **H1**·3MA, **H1**·4MA and 2(**H2**)·3(ANI)

	H1·3MA	**H1**·4MA	2(**H2**)·3(ANI)
Chemical formula	$C_{44}H_{36}N_2{\cdot}C_8H_{10}O$	$C_{44}H_{36}N_2{\cdot}C_8H_{10}O$	$2(C_{44}H_{40}N_2){\cdot}3(C_7H_8O)$
Formula weight	714.91	714.91	1517.96
Crystal system	Triclinic	Triclinic	Triclinic
Space group	$P\bar{1}$	$P\bar{1}$	$P\bar{1}$
μ (Mo-Kα)/mm^{-1}	0.070	0.071	0.071
a/Å	8.8540(4)	8.7789(5)	12.3235(7)
b/Å	10.4874(5)	10.3493(6)	13.4341(8)
c/Å	11.4956(6)	11.4397(6)	13.8154(8)
Alpha/°	96.485(2)	96.560 (2)	107.750(2)
Beta/°	102.370(2)	102.110 (2)	93.267(2)
Gamma/°	102.734(2)	102.726 (2)	102.939(2)
V/Å^3	1002.53(9)	977.14(10)	2103.6(2)
Z	1	1	1
D(calc)/g cm^{-1}	1.184	1.215	1.198
F(000)	380	380	810
Temp./K	296	200	296
Restraints	136	60	68
N_{ref}	4954	4816	10 394
N_{par}	282	283	558
R	0.0477	0.0411	0.0437
wR_2	0.1436	0.1129	0.1208
S	1.05	1.05	1.03
θ min – max/°	1.8, 28.3	1.8, 28.3	1.6, 28.3
Tot. data	35 289	36 097	73 977
Unique data	4954	4816	10 394
Observed data [$I > 2.0$ sigma(I)]	4009	4183	8283
R_{int}	0.020	0.019	0.017
Completeness	0.999	0.998	0.999
Min. resd. dens. (e/Å^3)	−0.31	−0.21	−0.17
Max. resd. dens. (e/Å^3)	0.30	0.31	0.28

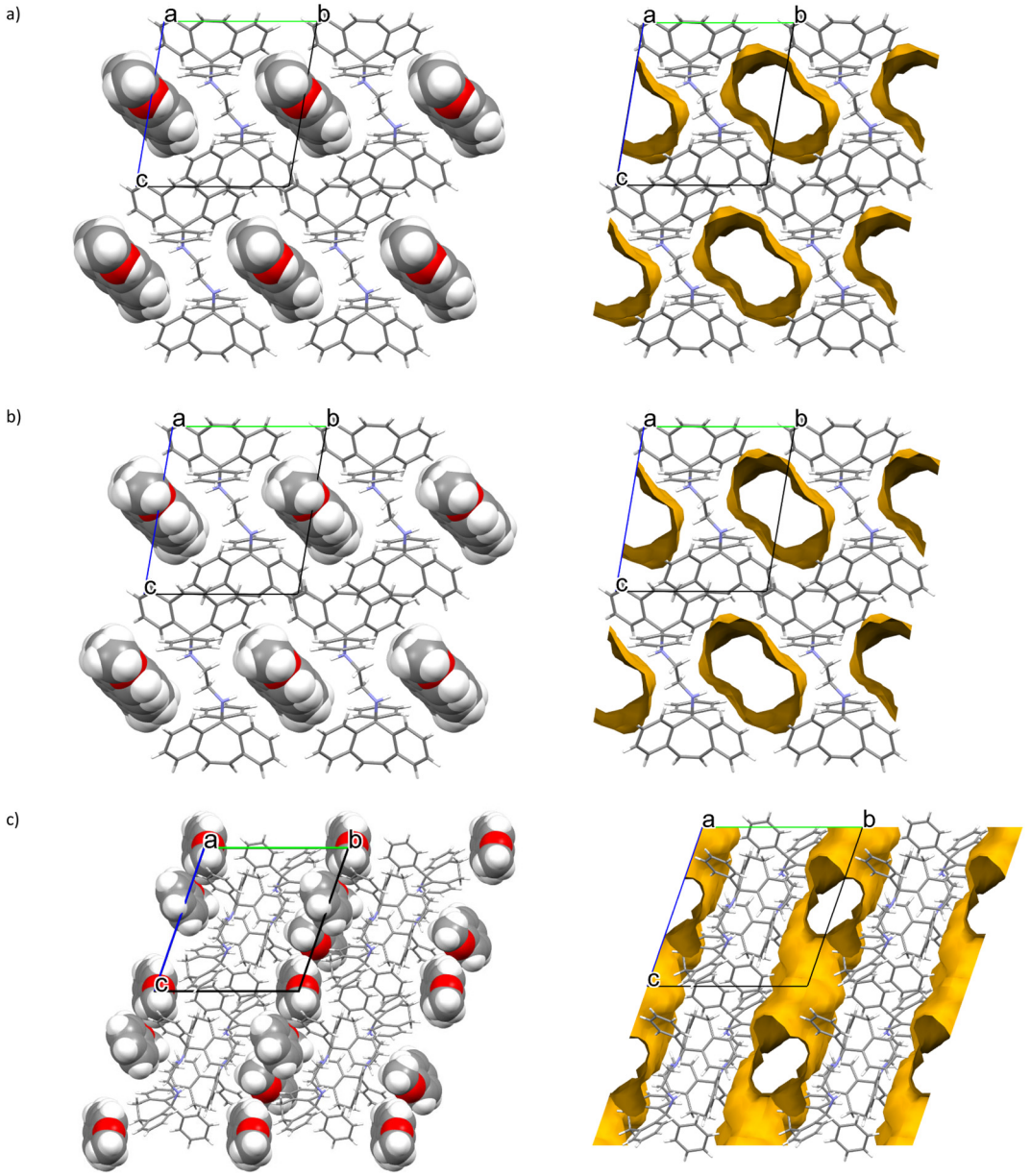

Fig. 2 Unit cells (left) and void diagrams (right) for a) **H1**·3MA, b) **H1**·4MA and c) 2(**H2**)·3(ANI).

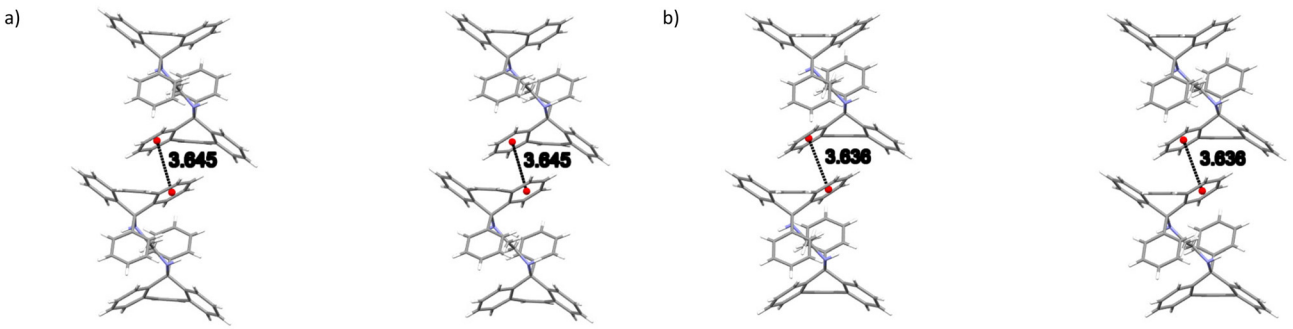

Fig. 3 Stereoviews of the intermolecular (host)π···π(host) interactions in a) **H1**·3MA and b) **H1**·4MA.

3MA. Furthermore, in **H1**·3MA were also observed four short intermolecular interactions, three of these between host and guest molecules, and one involving host molecules only. The first three interactions were of the (host)C–C···H–C (guest),

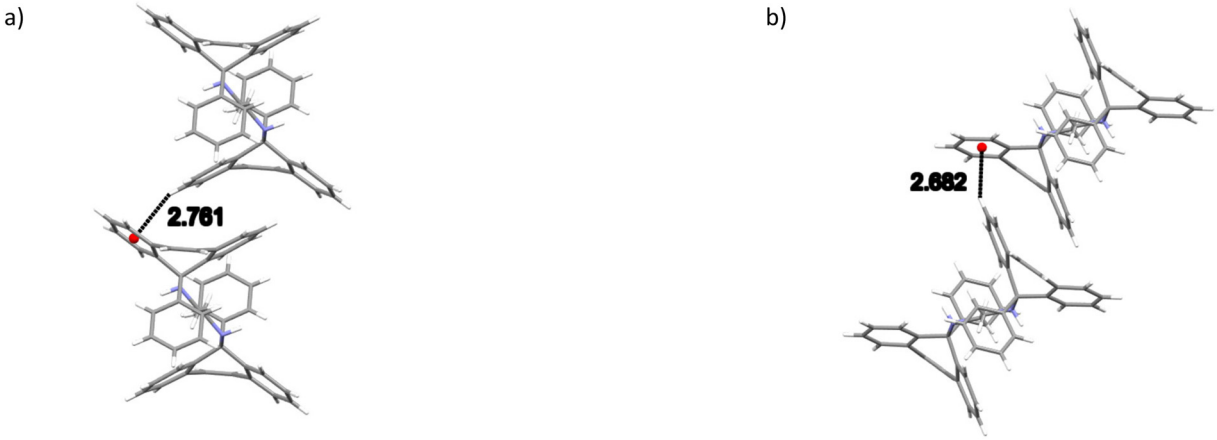

Fig. 4 Intermolecular (host)C–H···π(host) interactions in the a) **H1**·3MA and b) **H1**·4MA complexes.

(host)N–H···C–C(guest) and (host)C–H···H–C(guest) types, with distances and angles of 2.74 (118°), 2.89(2) (151.4(13)°) and 2.29 (156°) Å, respectively. The fourth was a (host)C–H···H–C(host) close contact that measured 2.21 Å (121°). **H1**·4MA, on the other hand, experienced three short intermolecular contacts but none of these were between host and guest molecules (this complex may thus be defined as a *true clathrate*): these (host)C–H···H–C(host), (host)C–H···C–C(host) and (guest)C–H···H–C(guest) interactions had distances of 2.16, 2.85 and 2.33 Å (119, 139 and 156°), respectively. Finally, in both complexes, two intramolecular non-classical hydrogen bonds were also identified. These were of the (host)C–H···N(host) type and, in all instances, measured 2.38 Å (with small angles, 104°).

In 2(**H2**)·3(ANI), two intramolecular (host)C–H···π(host) (2.99, 2.79 Å and 127, 141°, an example of which is provided in Fig. 5a) contacts, one intermolecular (host)C–H···π(host) (2.80 Å, 155°, Fig. 5b) contact and one intermolecular (guest) C–H···π(host) (2.75 Å, 167°, Fig. 5c) interaction were each identified. There were several other short intermolecular contacts as well, and their distances ranged between 2.62 and 2.87 Å (105–161°). Finally, both classical and non-classical intramolecular host···host hydrogen bonding interactions were also observed in this complex, with distances between 2.34 and 2.43 Å (102–113.8(11)°).

These SCXRD data have therefore demonstrated why 4MA was preferred by **H1** rather than 3MA (where higher crystal densities were noted in the 4MA-containing complex as a result of tighter packing which was facilitated by shorter intermolecular host···host contacts).

3.5 Thermal experiments

The thermogravimetric (TG), its derivative (DTG), and differential scanning calorimetric (DSC) traces are provided (overlaid) in Fig. 6a–c (**H1**) and 7 (**H2**), while the more important data from these traces are summarized in Table 5.

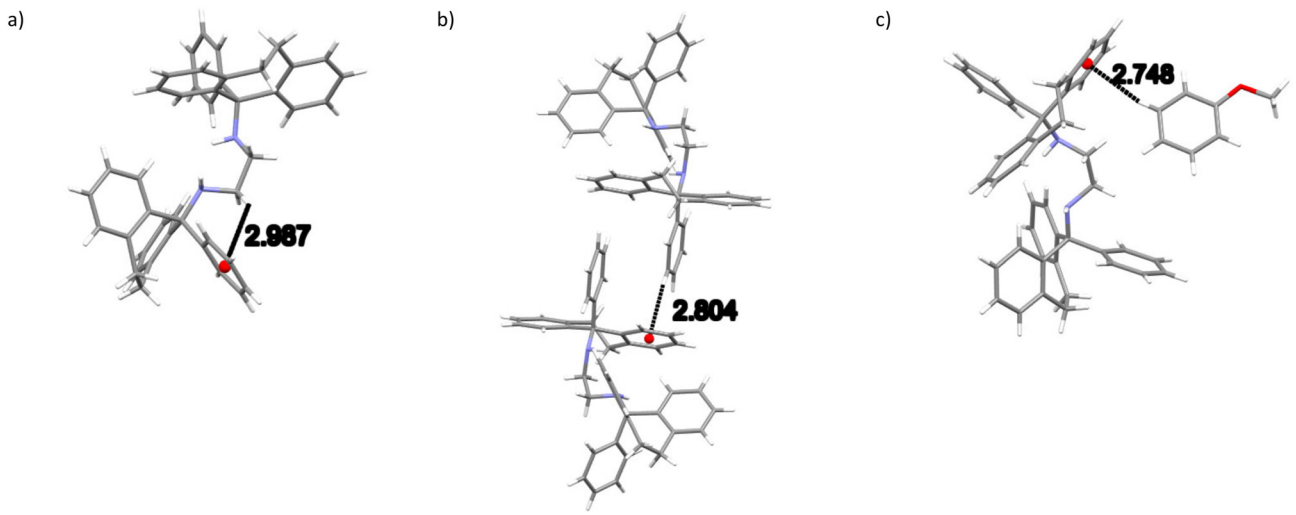

Fig. 5 Depiction of a) one of the intramolecular (host)C–H···π(host), b) the only intermolecular (host)C–H···π(host) and c) the only intermolecular (guest)C–H···π(host) interactions in 2(**H2**)·3(ANI).

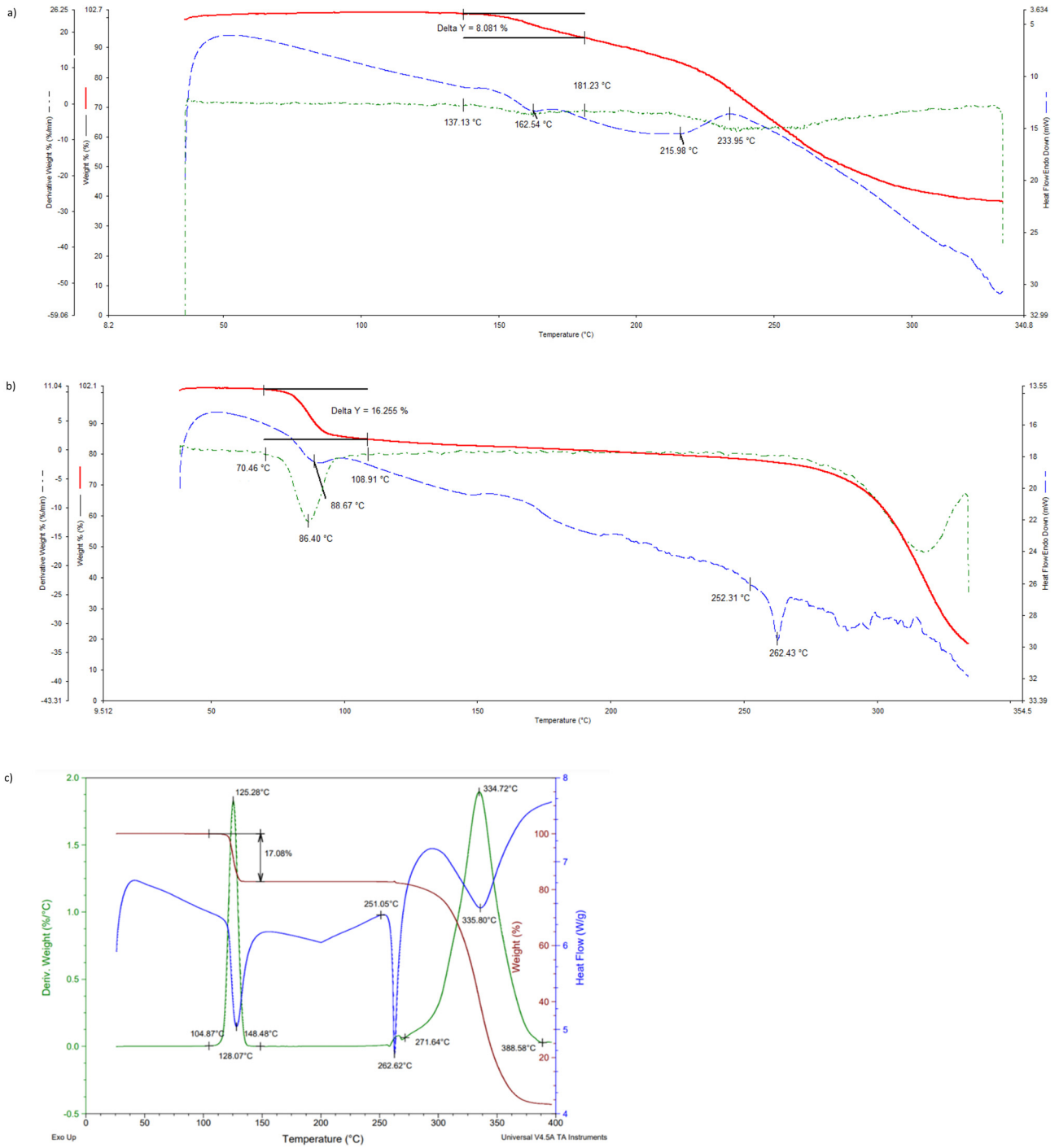

Fig. 6 Overlaid TG, DTG and DSC traces for a) 2(**H1**)·2MA, b) **H1**·3MA and c) **H1**·4MA.

If one compares the onset temperatures for the guest release process (T_{on}, which is a measure of the relative thermal stability of complexes) for **H1**·3MA and **H1**·4MA (Fig. 6b and c), it is clear that the latter inclusion compound is considerably more thermally stable than the former (T_{on} 104.9 compared with 70.5 °C) (Table 5). This is in accordance with the observations made in both the guest/guest competition (where 4MA was significantly preferred over 3MA) and the SCXRD (where crystals of the 4-MA-containing complex possessed a higher density and shorter intermolecular host···host interactions than that containing 3MA) experiments. In both complexes, the guest release is *via* a single step, and expected and calculated mass loss measurements concurred closely (expected 17.1%, observed 16.3 and 17.1%, respectively). These guest release processes were then followed by the host melt endotherm which commenced at 252.3 and 251.1 °C, and which is in agreement with the literature (255 °C (ref. 20)). It is

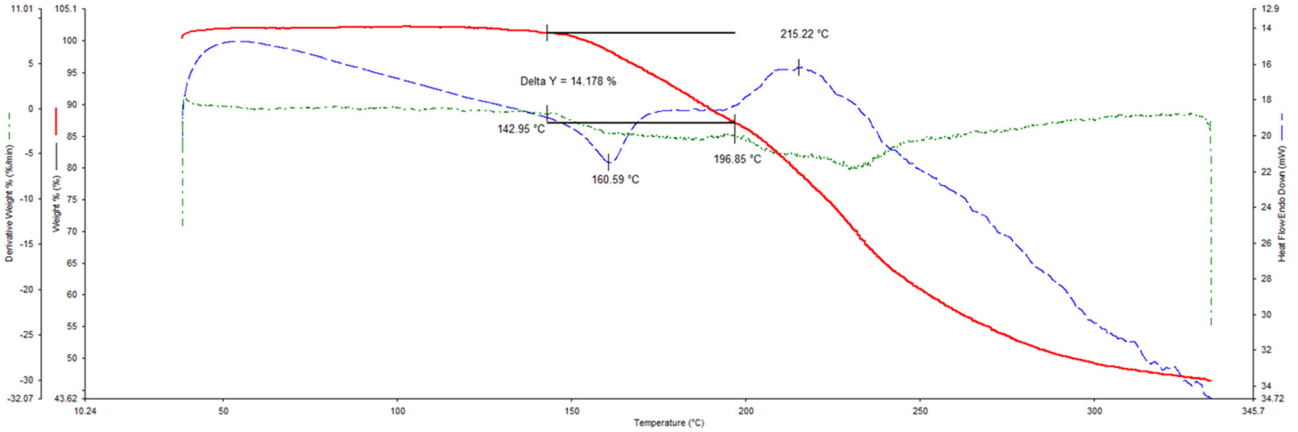

Fig. 7 Overlaid TG, DTG and DSC traces for 2(**H2**)·3(ANI).

Table 5 Thermal data for the 2(**H1**)·2MA, **H1**·3MA, **H1**·4MA and 2(**H2**)·3(ANI) complexes

Complex	T_{on}/°C[a]	Calculated mass loss/%	Experimental mass loss/%
2(**H1**)·2MA	136.1	9.5	8.1
H1·3MA	70.5	17.1	16.3
H1·4MA	104.9	17.1	17.1
2(**H2**)·3(ANI)	[b]	21.4	14.2[b]

[a] T_{on} is the onset temperature for the guest release process and a measure of the thermal stability of the complex, and was estimated from the DTG/TG. [b] Some guest escaped from the crystals during sample preparation.

unfortunate that 2(**H1**)·2MA crystallized out as a powder and therefore that the reason for its high thermal stability (T_{on} 136.1 °C) could not be established since a SCXRD experiment was not possible. However, it must be noted that the thermal trace for this complex was not unambiguous (Fig. 6a): while the expected mass loss (9.5%) was in reasonable agreement with that measured (8.1%), the guest release and host melt events are not obvious in this figure.

In the case of the 2(**H2**)·3(ANI) complex, the expected (21.4%) and measured (14.2%) mass losses differed significantly (Fig. 7, Table 5). It is proposed that some of the anisole guest escaped from its channels in the crystals of the complex during the preparation of the sample for thermal analysis, and so the mass loss measured was much lower than required for this 2 : 3 H : G complex. Once more, the host melt endotherm is not obvious in this figure (the literature melting point of **H2** is between 186 and 187 °C (ref. 20)).

4. Conclusion

In this work, it was demonstrated that **H1** possessed a high affinity for 4MA in mixtures containing this guest, even though both 2MA and 3MA were also enclathrated in the single solvent recrystallization experiments: the H : G ratios were 2 : 1 (2MA) and 1 : 1 (for both 3MA and 4MA). In the crystals obtained from equimolar binary ANI/4MA, 2MA/4MA and 3MA/4MA solutions were measured between 84.4 and 91.7% 4MA. Remarkably, in the absence of 4MA, only apohost compound was recovered from the glass vessels. Selectivity profiles obtained from the 4MA/ANI, 4MA/2MA and 4MA/3MA experiments revealed that 4MA was consistently preferred across the concentration range, but that the K_{ave} values (3.4–6.1) were not high enough to suggest that **H1** would be a suitable host candidate for these anisole separations. SCXRD experiments revealed the reasons for the affinity of **H1** for 4MA relative to 3MA: the intermolecular host···host C–H···π and π···π interactions in the complex containing the preferred guest (4MA) were significantly shorter than in the complex with 3MA (note that no host···guest interactions were observed in **H1**·4MA, and this complex was therefore described as a *true clathrate*). This, in turn, led to a higher crystal density in **H1**·4MA (1.215 g cm^{-1}) compared with **H1**·3MA (1.184 g cm^{-1}) despite their identical chemical formulae, and this implies that the complex with 4MA experiences a tighter and more stabilized host packing. This was confirmed by thermal analyses: the onset temperature for the guest release process for **H1**·4MA (104.9 °C) was much higher than for **H1**·3MA (70.5 °C). Both guest compounds, however, were observed to reside in wide open channels. Unfortunately, the 2MA-containing complex crystallized out as a powder and SCXRD analyses could not be employed in order to understand the guest retention mode in the crystals. This complex, however, experienced a high T_{on}, 136.1 °C, despite 2MA being significantly less preferred by **H1** than 4MA (T_{on} = 104.9 °C). Finally, the thermal traces for 2(**H1**)·2MA were not unambiguous and the host melt endotherm could not be clearly discerned on the DSC trace. Unfortunately, **H2** only complexed with ANI, and no guest/guest competition experiments could be carried out owing to the fact that crystallization was

unsuccessful for **H2** from these mixed guests. However, ANI was observed to be held in the crystals of the complex by means of a number of short contacts by SCXRD experiments. Despite this, the complex stability remained low since some guest escaped from the crystals at ambient conditions during sample preparation for thermal analysis.

Author contributions

Benita Barton: conceptualization; funding acquisition; methodology; project administration; resources; supervision; visualization; writing – original draft. Danica B. Trollip: investigation; methodology; validation. Eric C. Hosten: data curation; formal analysis.

Conflicts of interest

There are no conflicts of interest to declare.

Acknowledgements

Financial support is acknowledged from the Nelson Mandela University and the National Research Foundation (NRF) of South Africa (NRF Grant number UID 144918).

References

1 PubChem/Anisole/Nih.gov., **https://pubchem.ncbi.nlm.nih.gov/compound/Anisole** (accessed 2022-11-18).
2 D. Dang, Z. Wang, W. Lin and W. Song, Synthesis of anisole by vapor phase methylation of phenol with methanol over catalysts supported on activated alumina, *Chin. J. Catal.*, 2016, **37**, 720–726.
3 Y. Wu, Y. Huang, H. Huang, Y. Muhammad, Z. Huang, J. Winarta, Y. Zhang, S. Nie, Z. Zhao and B. Mu, Porous Fe@C composites derived from silkworm excrement for effective separation of anisole compounds, *ACS Omega*, 2019, **4**, 21204–21213.
4 S. Balsama, P. Beltrame, P. L. Beltrame, P. Carniti, L. Forni and G. Zuretti, Alkylation of phenol with methanol over zeolites, *Appl. Catal.*, 1984, **13**, 161–170.
5 F. Huang, L. Li, M. Guan, Z. Hong, L. Miao, G. Zhao and Z. Zhu, A review of the process on vapor phase methylation of phenol with methanol, *Catal. Lett.*, 2023, **153**, 754–769.
6 B. Barton, M. R. Caira, U. Senekal and E. C. Hosten, Selectivity considerations of the roof-shaped host compound trans-α,α,α′,α′-tetrakis(4-chlorophenyl)-9,10-dihydro-9,10-ethanoanthracene-11,12-dimethanol in mixed anisoles, *Cryst. Growth Des.*, 2022, **22**, 6818–6826.
7 S. Fanali, Separation of optical isomers by capillary zone electrophoresis based on host-guest complexation with cyclodextrins, *J. Chromatogr.*, 1989, **474**, 441–446.
8 M. D. Ward and A. M. Pivovar, Organic host-guest molecular assemblies, *Curr. Opin. Solid State Mater. Sci.*, 1999, **4**, 581–586.
9 E. Alvira, J. I. García and J. A. Mayoral, Molecular modelling study for chiral separation of equol enantiomers by β-cyclodextrin, *Chem. Phys.*, 1999, **240**, 101–108.
10 S. Fanali and M. Sinibaldi, Host-guest complexation in capillary isotachophoresis: 1. α-, β- and λ-cyclodextrins as complexing agents for the resolution of substituted benzoic acid isomers, *J. Chromatogr.*, 1988, **442**, 371–377.
11 F. Toda, Chapter IV.3 Isolation of isomers and optical resolution by a host-guest complexation method, *Stud. Surf. Sci. Catal.*, 1990, **54**, 340–351.
12 G. Zhang, A.-H. Emwas, U. F. S. Hameed, S. T. Arold, P. Yang, A. Chen, J.-F. Xiang and N. M. Khashab, Shape-induced selective separation of ortho-substituted benzene isomers enabled by cucurbit[7]uril host macrocycles, *Chem*, 2020, **6**, 1082–1096.
13 M. Lusi and L. J. Barbour, Solid–vapor sorption of xylenes: prioritized selectivity as a means of separating all three isomers using a single substrate, *Angew. Chem., Int. Ed.*, 2012, **51**, 3928–3931.
14 N. M. Sykes, H. Su, E. Weber, S. A. Bourne and L. R. Nassimbeni, Selective enclathration of methyl- and dimethylpiperidines by fluorenol hosts, *Cryst. Growth Des.*, 2017, **17**, 819–826.
15 B. Barton, U. Senekal and E. C. Hosten, Host compound DED: guest accommodation type, noncovalent host···guest interactions, crystal densities, and thermal stabilities ensure high host selectivities for 4-methylanisole in anisole and methylanisole mixtures, *Cryst. Growth Des.*, 2023, **23**, 602–611.
16 B. Barton, P. L. Pohl and E. C. Hosten, Complexes of host compound (−)-(2R,3R)-2,3-dimethoxy-1,1,4,4-tetraphenylbutane-1,4-diol (DMT) with guests anisole and the methyl-substituted anisoles: host selectivity, thermal and single crystal diffraction considerations, *J. Inclusion Phenom. Macrocyclic Chem.*, 2018, **92**, 357–367.
17 J. L. Atwood and J. W. Steed, *Encyclopedia of Supramolecular Chemistry*, CRC Press, Marcel Dekker, Inc., New York, 2004, vol. 1.
18 J. W. Steed and J. L. Atwood, *Supramolecular Chemistry*, John Wiley & Sons, Ltd., USA, 2009.
19 B. Barton, D. B. Trollip and E. C. Hosten, Selected tricyclic fused systems: host behaviour in the presence of mixed xylenes and ethylbenzene, *Cryst. Growth Des.*, 2022, **22**, 6726–6734.
20 B. Barton, R. Betz, M. R. Caira, E. C. Hosten, C. W. McCleland, P. L. Pohl and B. Taljaard, Clathrates of novel ethylenediamine derivatives: thermal, X-ray crystallographic and conformational analysis of inclusion complexes of N,N′-bis(5-phenyl-5-dibenzo[a,d]cycloheptenyl)ethylenediamine and its 10,11-dihydro analogue, *Tetrahedron*, 2016, **72**, 7536–7551.
21 Bruker A., *APEX2, SADABS and SAINT*, Bruker AXS, Madison, 2010.
22 G. M. Sheldrick, SHELXT–Integrated space-group and crystal-structure determination, *Acta Crystallogr., Sect. A: Found. Adv.*, 2015, **71**, 3–8.

23 G. M. Sheldrick, Crystal structure refinement with SHELXL, *Acta Crystallogr., Sect. C: Struct. Chem.*, 2015, **71**, 3–8.
24 C. B. Hübschle, G. M. Sheldrick and B. Dittrich, ShelXle: a Qt graphical user interface for SHELXL, *J. Appl. Crystallogr.*, 2011, **44**, 1281–1284.
25 A. M. Pivovar, K. T. Holman and M. D. Ward, Shape-selective separation of molecular isomers with tunable hydrogen-bonded host frameworks, *Chem. Mater.*, 2001, **13**, 3018–3031.
26 C. F. Macrae, I. Sovago, S. J. Cottrell, P. T. A. Galek, P. McCabe, E. Pidcock, M. Platings, G. P. Shields, J. S. Stevens, M. Towler and P. A. Wood, Mercury 4.0: from visualization to analysis. Design and prediction, *J. Appl. Crystallogr.*, 2020, **53**, 226–235.
27 N. M. Sykes, H. Su, E. Weber, S. A. Bourne and L. R. Nassimbeni, Selective Enclathration of methyl- and dimethylpiperidines by fluorenol hosts, *Cryst. Growth Des.*, 2017, **17**, 819–826.

